Supporting Information

TopoChip-Based High-Throughput Screening of Micropatterned Hydroxyapatite to Guide Stem Cell Behavior and Accelerate Bone Regeneration

Yada Li[a, b], Chuanxin Zhong[a], Mingyu Zhu[a], Qiming Zhuang[a], Yuqi Tang[a], Jianfeng Yan[a], Ju Fang[a, *], Xiang Ge[c], Fuzeng Ren[a, *]

[a] Department of Materials Science and Engineering, Southern University of Science and Technology, Shenzhen, Guangdong 518055, China

[b] Department of Orthopaedics, Affiliated Zhongshan Hospital of Dalian University, Dalian 116001, China

[c] Key Laboratory of Mechanism Theory and Equipment Design of Ministry of Education, School of Mechanical Engineering, Tianjin University, Tianjin 300354, China

[*] Corresponding author. E-mail: fangj@sustech.edu.cn (J. F.), renfz@sustech.edu.cn (F. R.).

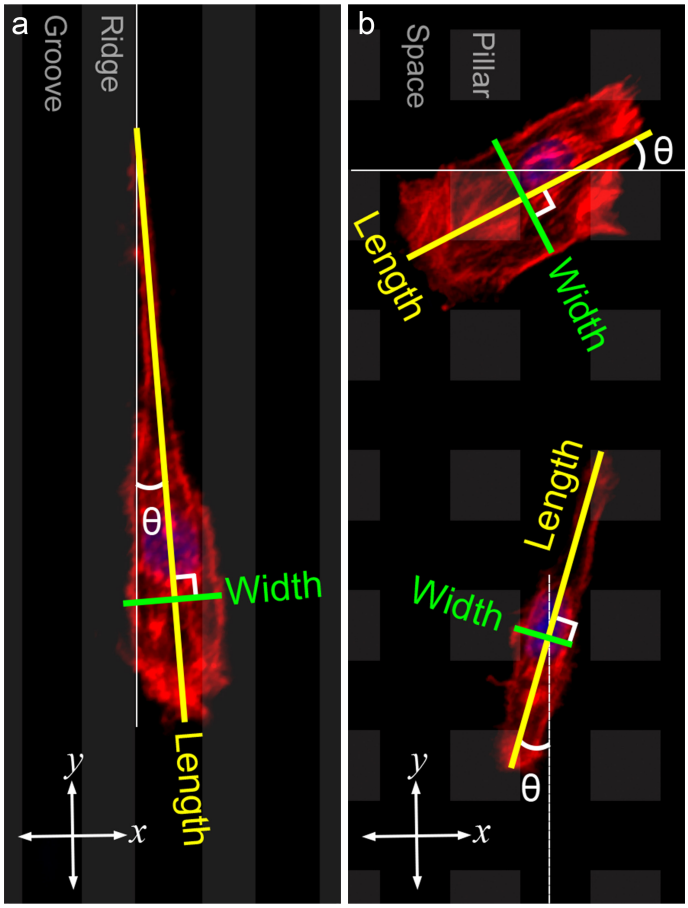

Fig. S1. Schematic illustrations of the measurement of cellular length, width, and orientation angle, along with the *x* and *y* axes of the patterns: (a) groove pattern, (b) pillar pattern.

Table S1. Genes and primers used in qPCR.

Gene	Primer Sequence
Vinculin	F: 5'-ATTGACGCTGCGCAGAATTG-3'
	R: 5'-CAAAGCCCCTCGGATCTGTT-3'
Integrin α5	F: 5'-AGCTGCATTTCCGAGTCTG-3'
	R: 5'-CTCACACTGAAGGCTGAACG-3'
Integrin β1	F: 5'-GGACGCTGCGAAAAGATGAA-3'
	R: 5'-CACATCGTGCAGAAGTAGGC-3'
RUNX2	F: 5'-CAGTATGAGAGTAGGTGTCCCGC-3'
	R: 5'-AAGAGGGGTAAGACTGGTCATAGG-3'
ALP	F: 5'-TCCATGGTGGATTATGCTCA-3'
	R: 5'-TTCTGTTCCTGCTCGAGGTT-3'
OCN	F: 5'-AGGGCAGTAAGGTGGTGAATAGA-3'
	R: 5'-GAAGCCAATGTGGTCCGCTA-3'
OPN	F: 5'-GAGTTTGGCAGCTCAGAGGA-3'
	R: 5'-TCTGCTTCTGAGATGGGTCA-3'
GAPDH	F: 5'-TTCCTACCCCCAATGTATCCG-3'
	R: 5'-CATGAGGTCCACCACCCTGTT-3'

F: forward, R: reverse.

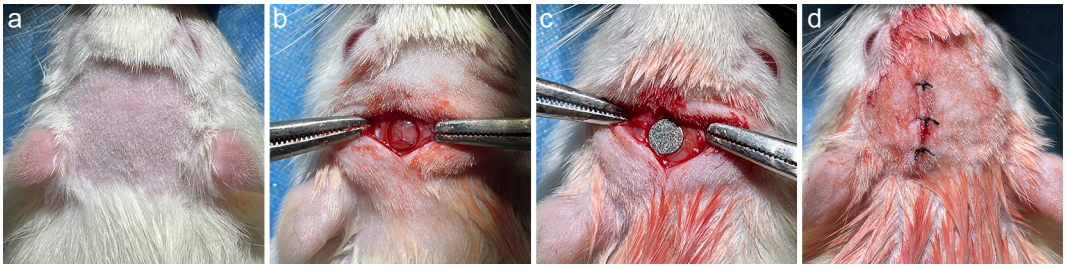

Fig. S2. Photos of surgery procedures. (a) hair shaved, (b) incision and defect created, (c) sample disk implanted in the defect, (d) incision sutured.

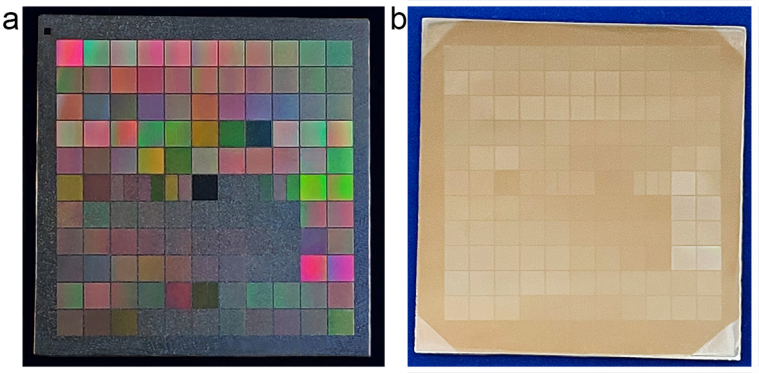

Fig. S3. Photos of the micropatterned Ti (a) and HA (b) TopoChips.

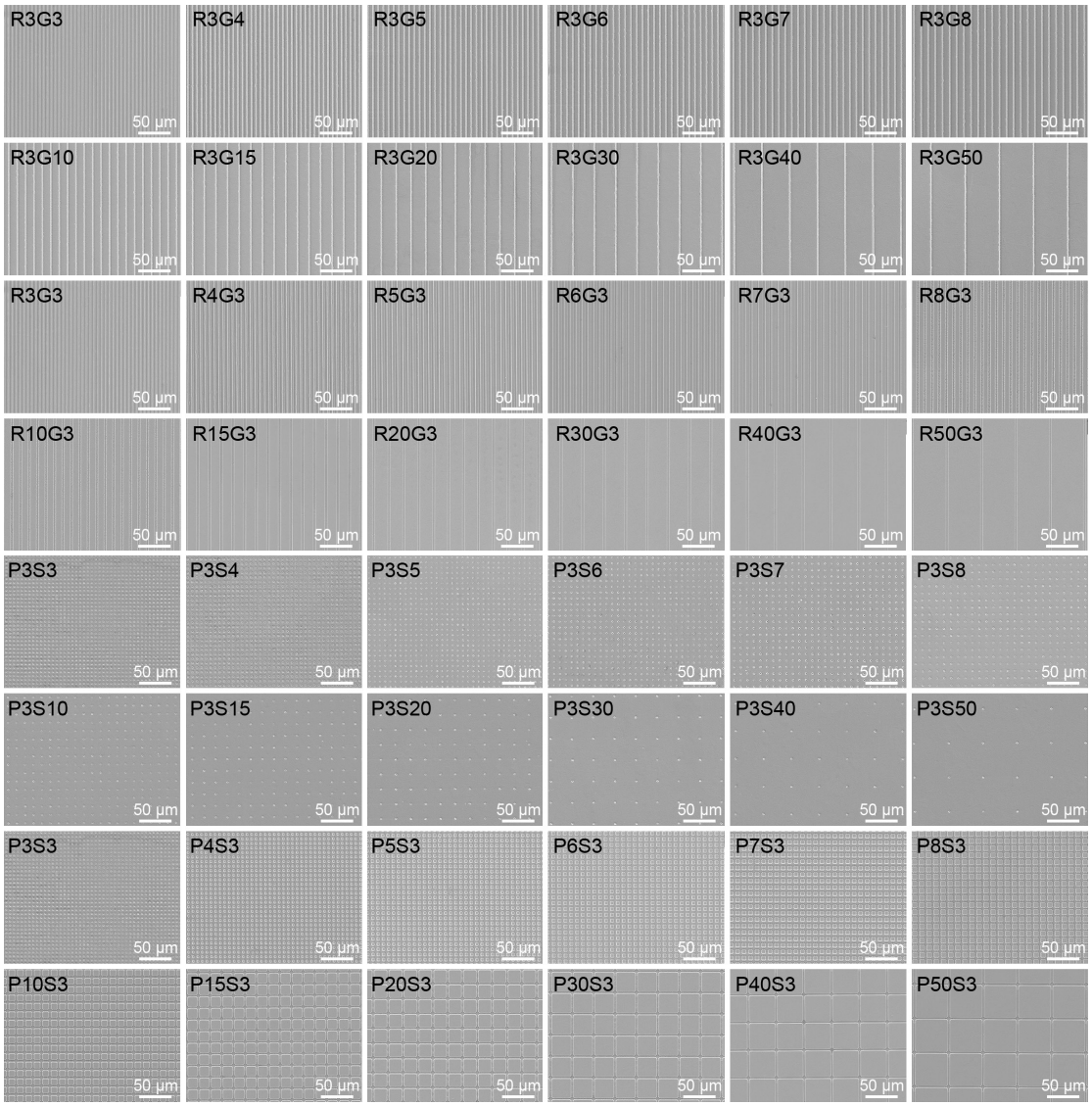

Fig. S4. SEM images of representative micropatterns of the Ti TopoChip: R3, G3, P3, and S3.

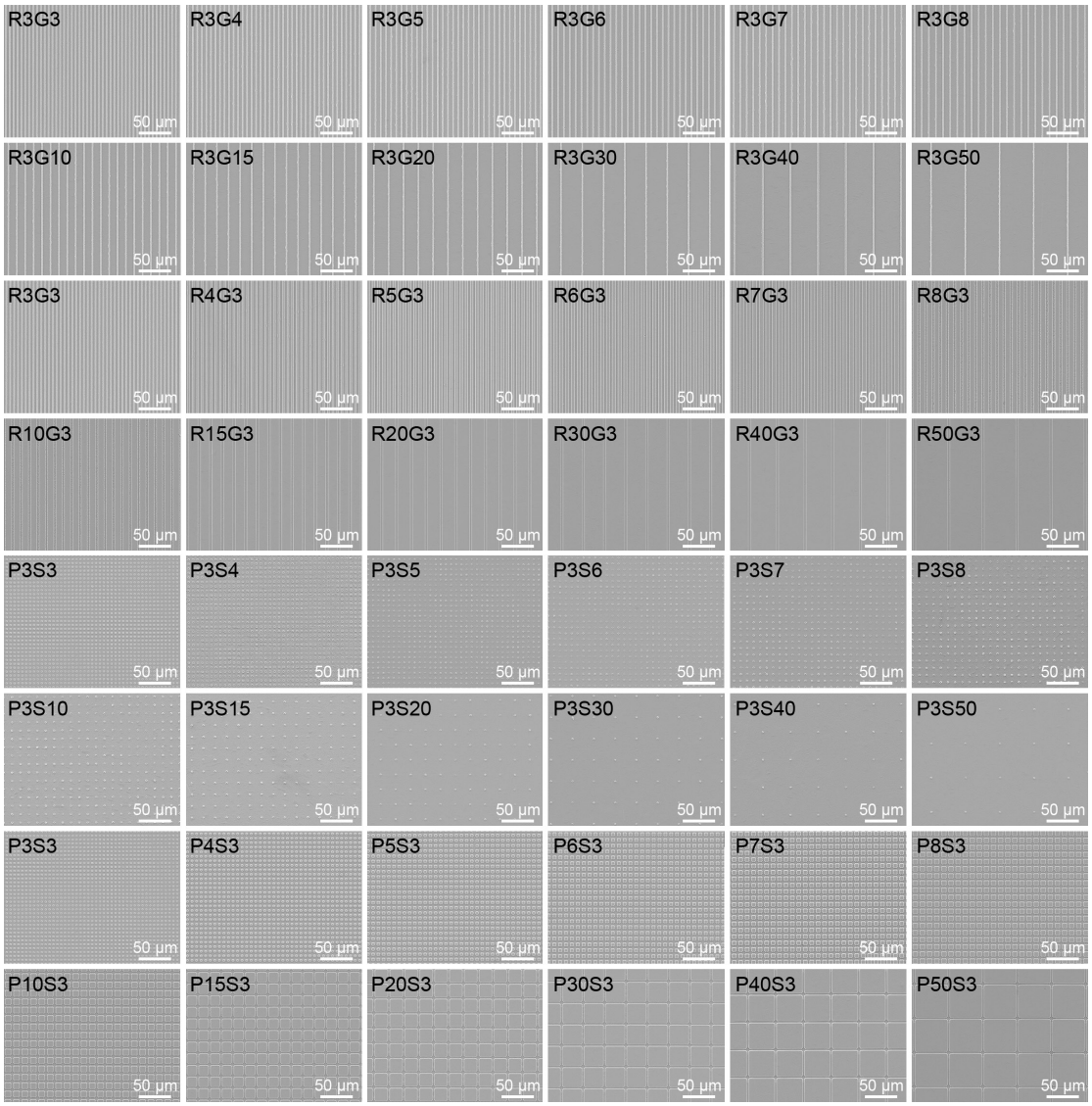

Fig. S5. SEM images of representative micropatterns of the HA TopoChip: R3, G3, P3, and S3.

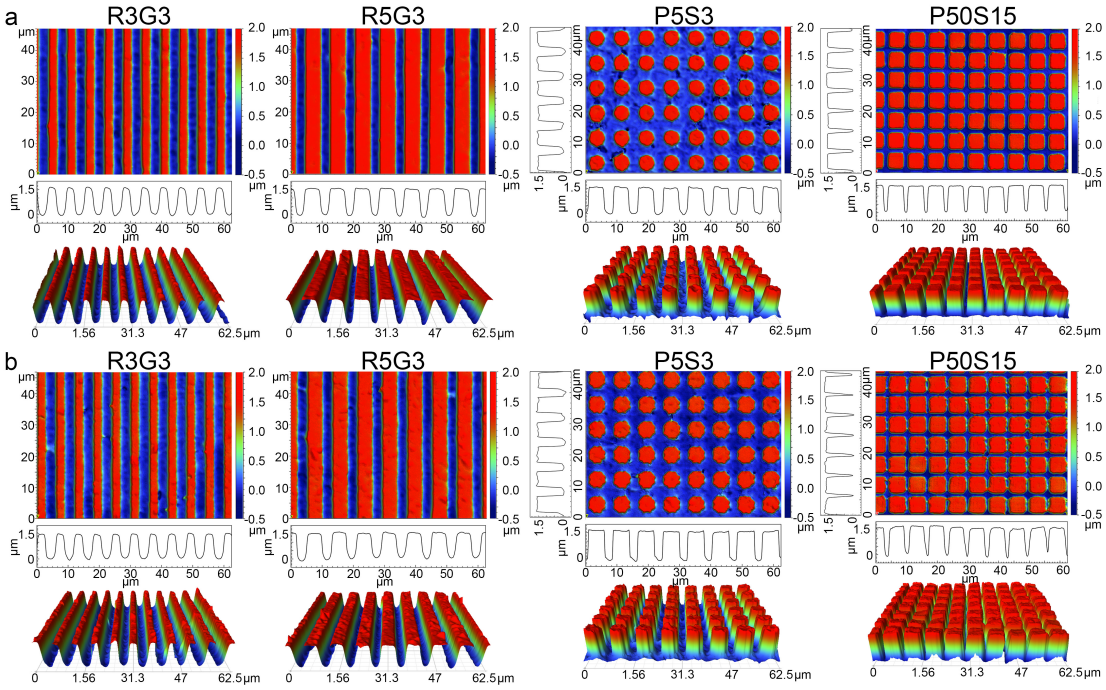

Fig. S6. Two-dimensional pseudo-color images and cross-sectional profiles of surface height, and three-dimensional surface profiles of representative micropatterns of the Ti (a) and HA (b) TopoChips.

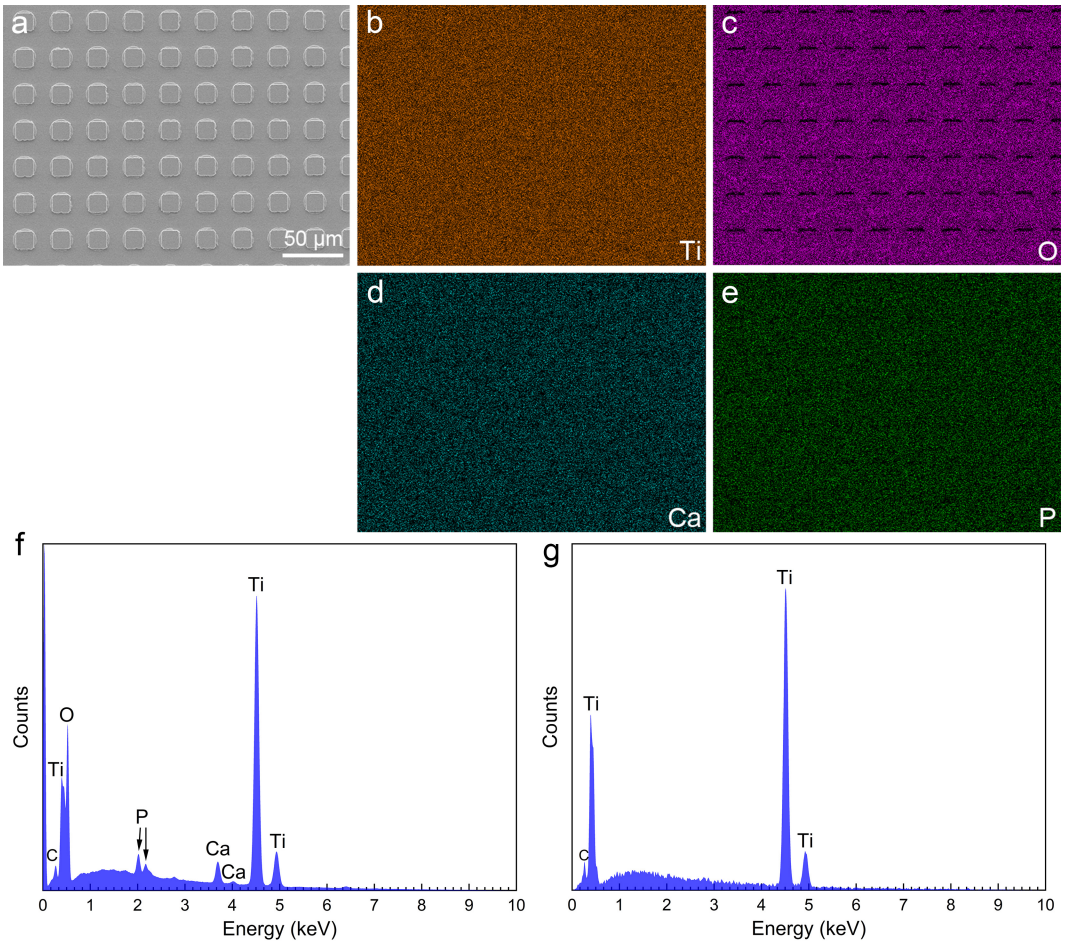

Fig. S7. SEM image of the HA-coated P15S15 (a) and the corresponding EDS elemental maps (b–e) and spectrum (f), and EDS spectrum of the Ti TopoChip (g).

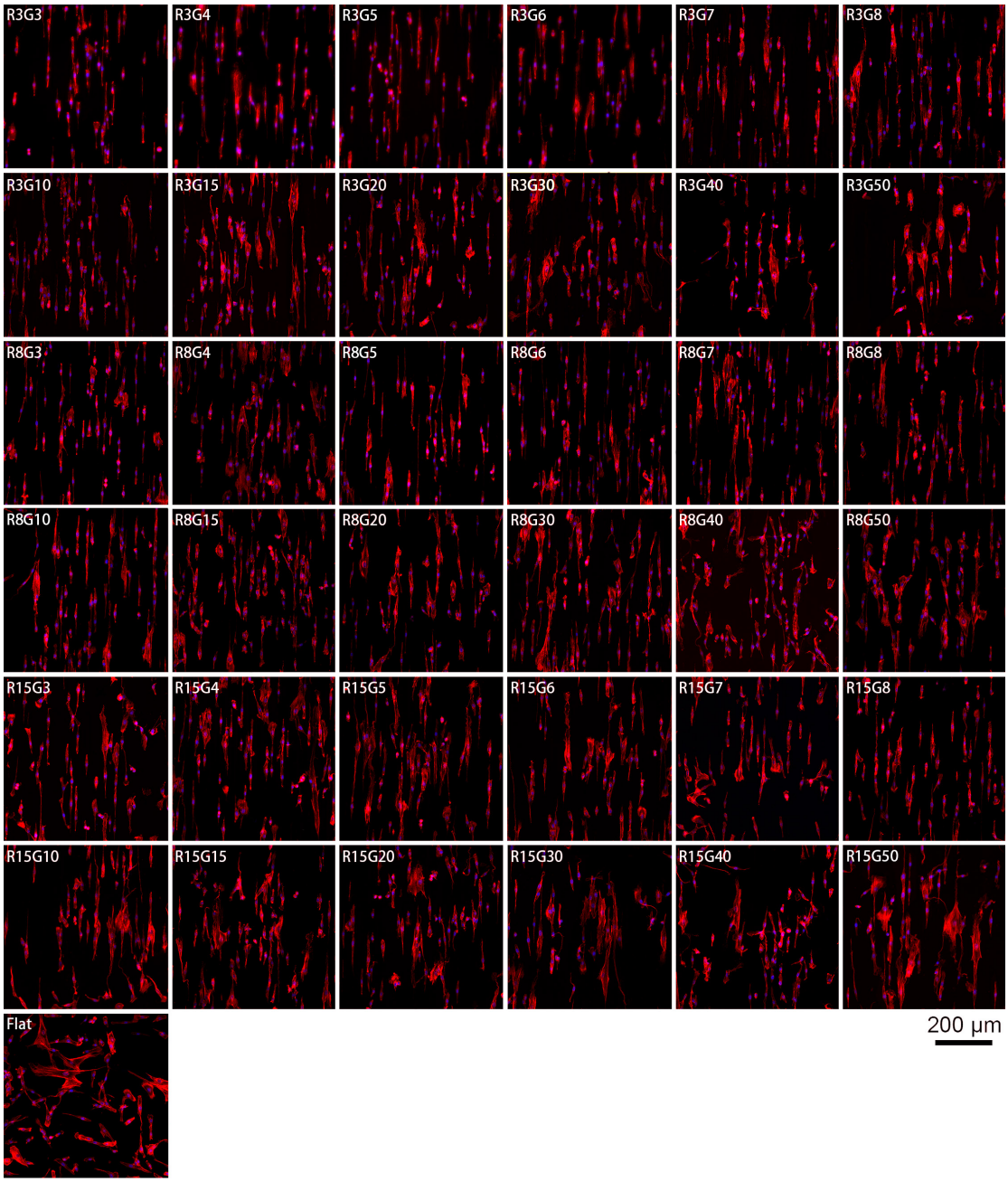

Fig. S8. Morphology images of cells on Flat and microgroove patterns with a fixed ridge width of 3, 8, and 15 μm, i.e., R3, R8, and R15.

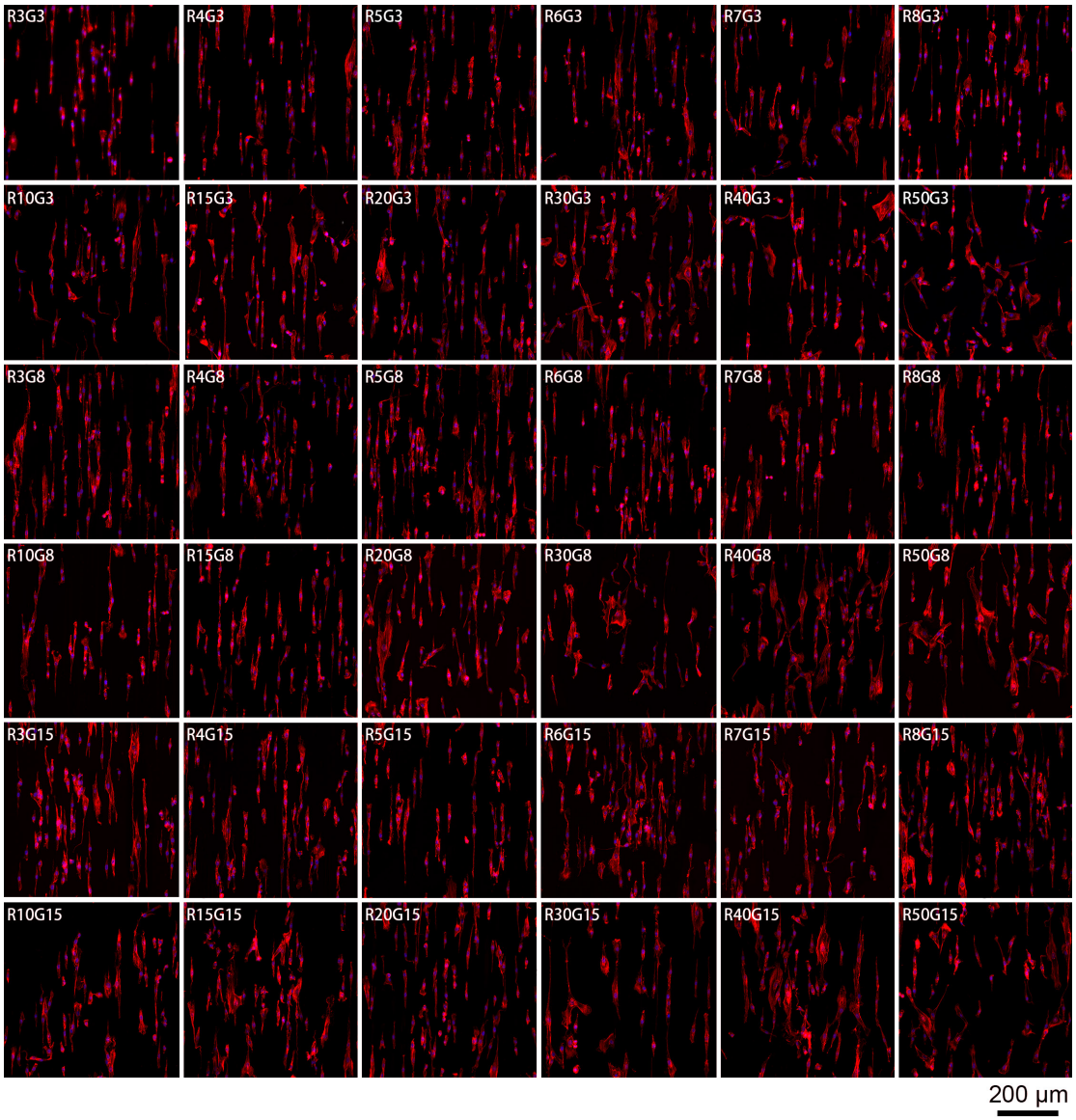

Fig. S9. Morphology images of cells on the microgroove patterns with a fixed groove width of 3, 8, and 15 μm, i.e., G3, G8, and G15.

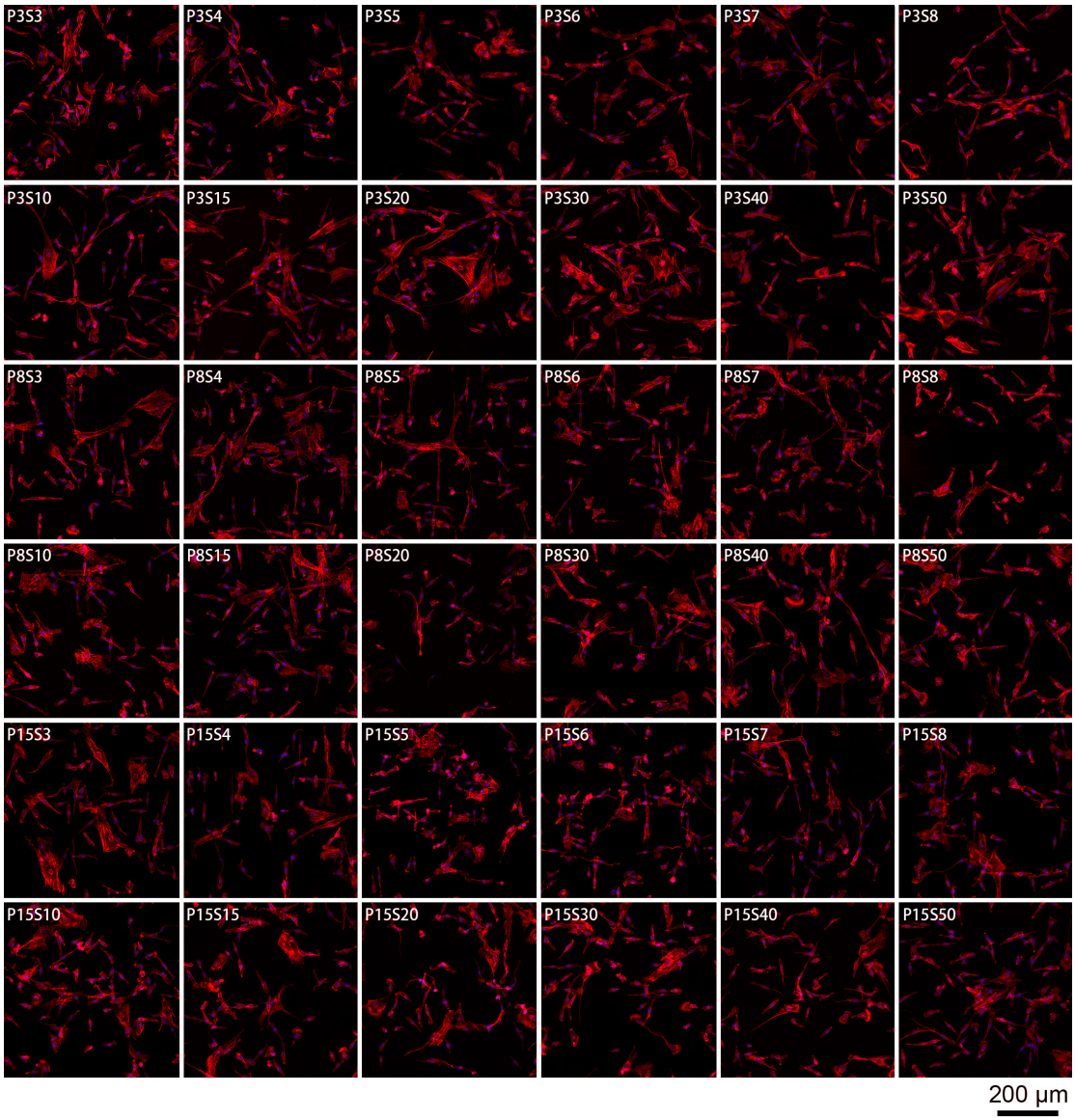

Fig. S10. Morphology images of cells on the micropillar patterns with a fixed pillar width of 3, 8, and 15 μm, i.e., P3, P8, and P15.

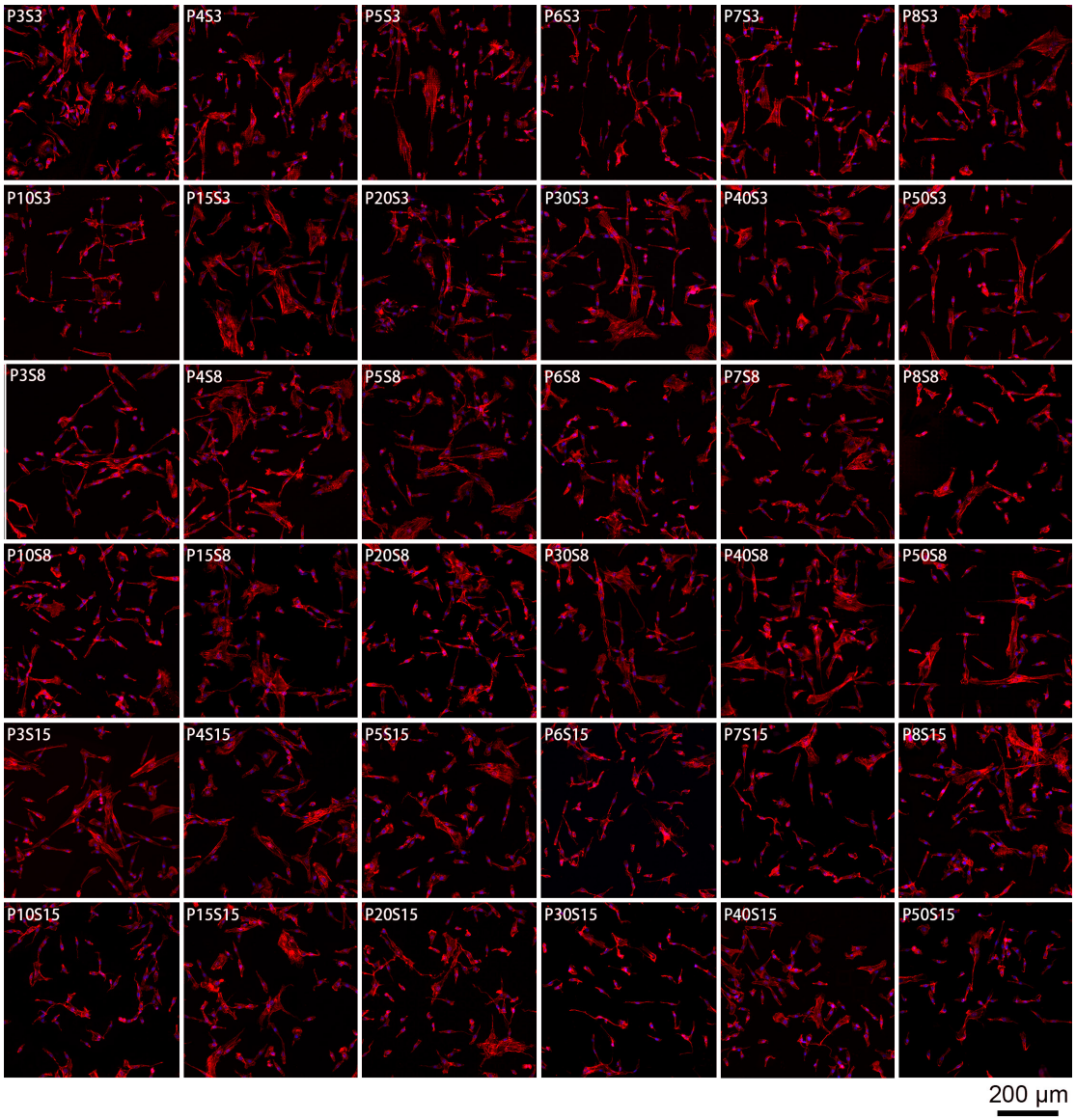

Fig. S11. Morphology images of cells on the micropillar patterns with a fixed space width of 3, 8, and 15 μm, i.e., S3, S8, and S15.

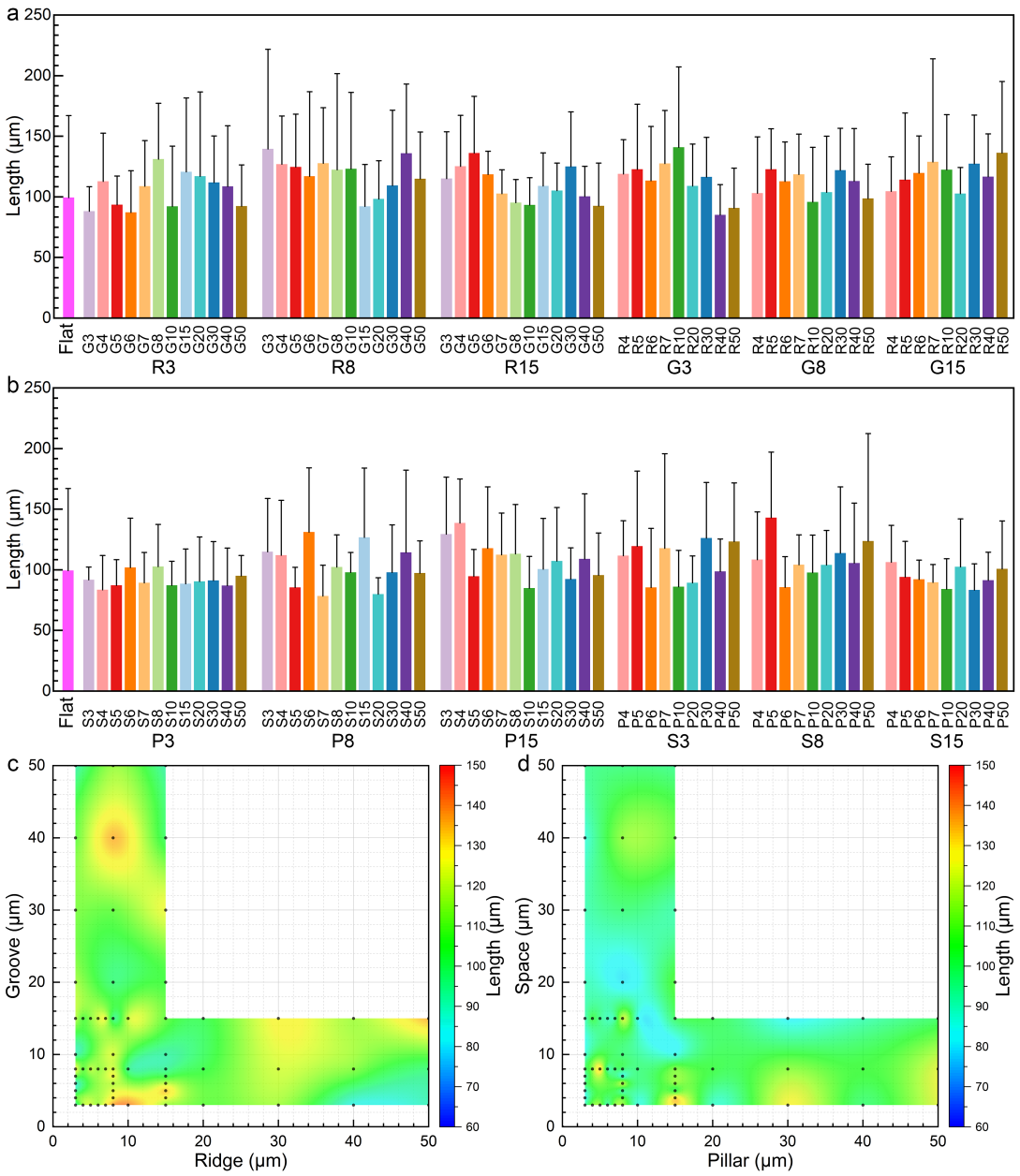

Fig. S12. Length of the cells on each pattern of the HA TopoChip (a, b) and the corresponding contour maps (c, d): (a, c) microgrooves, (b, d) micropillars. $n = 10$.

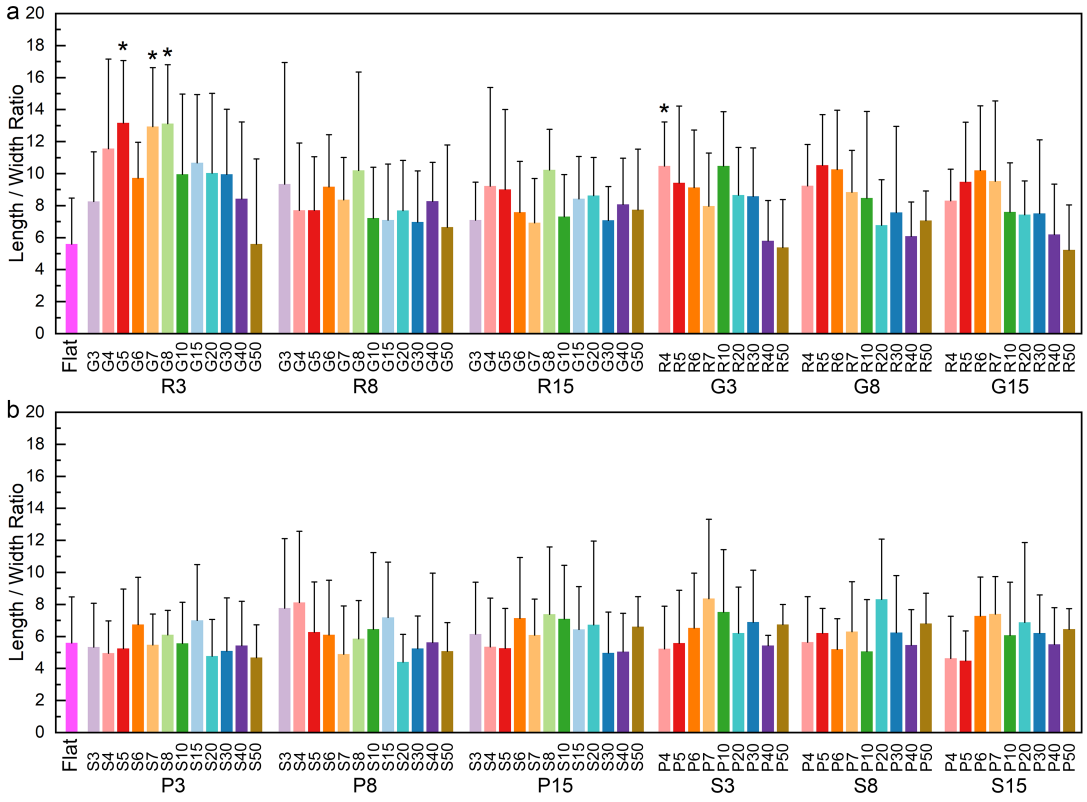

Fig. S13. Elongation of the cells on each pattern of the HA TopoChip: (a) microgrooves, (b) micropillars. $n = 10$, * $p < 0.05$.

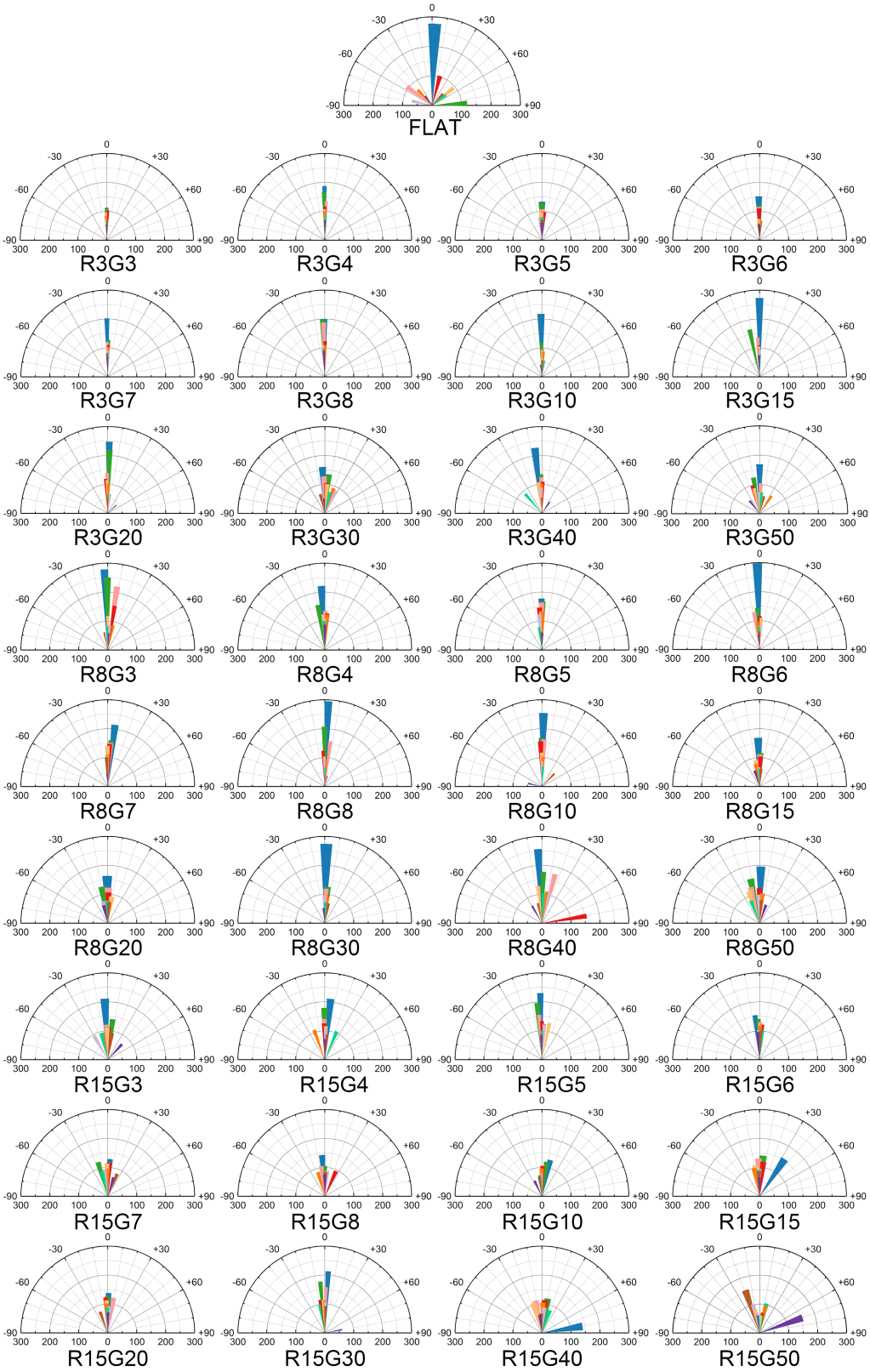

Fig. S14. Polar plots of the orientation angle with the cellular length (μm) of the cells on Flat and microgroove patterns with a fixed ridge width of 3, 8, and 15 μm, i.e., R3, R8, and R15.

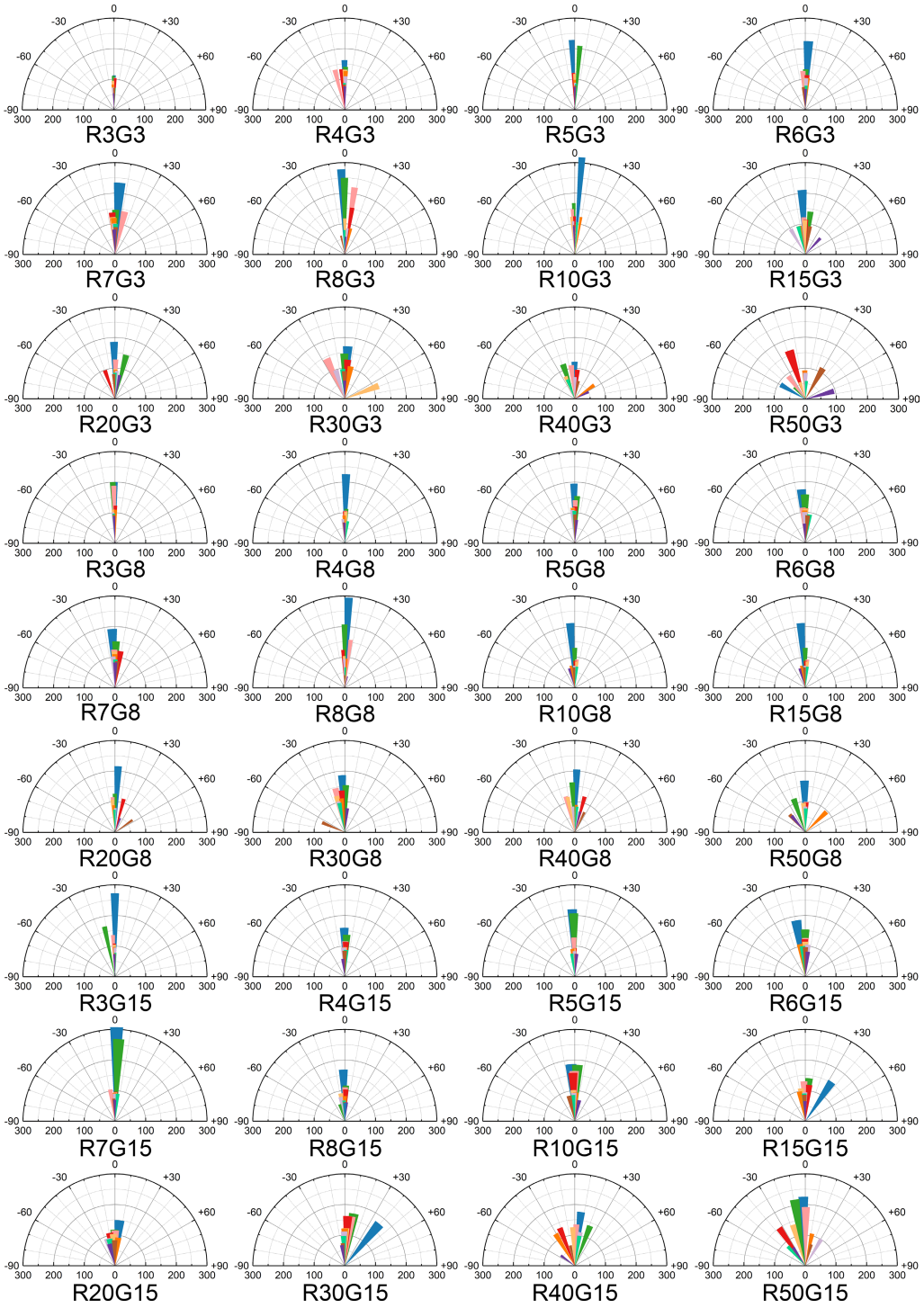

Fig. S15. Polar plots of the orientation angle with the cellular length (μm) of the cells on the microgroove patterns with a fixed groove width of 3, 8, and 15 μm, i.e., G3, G8, and G15.

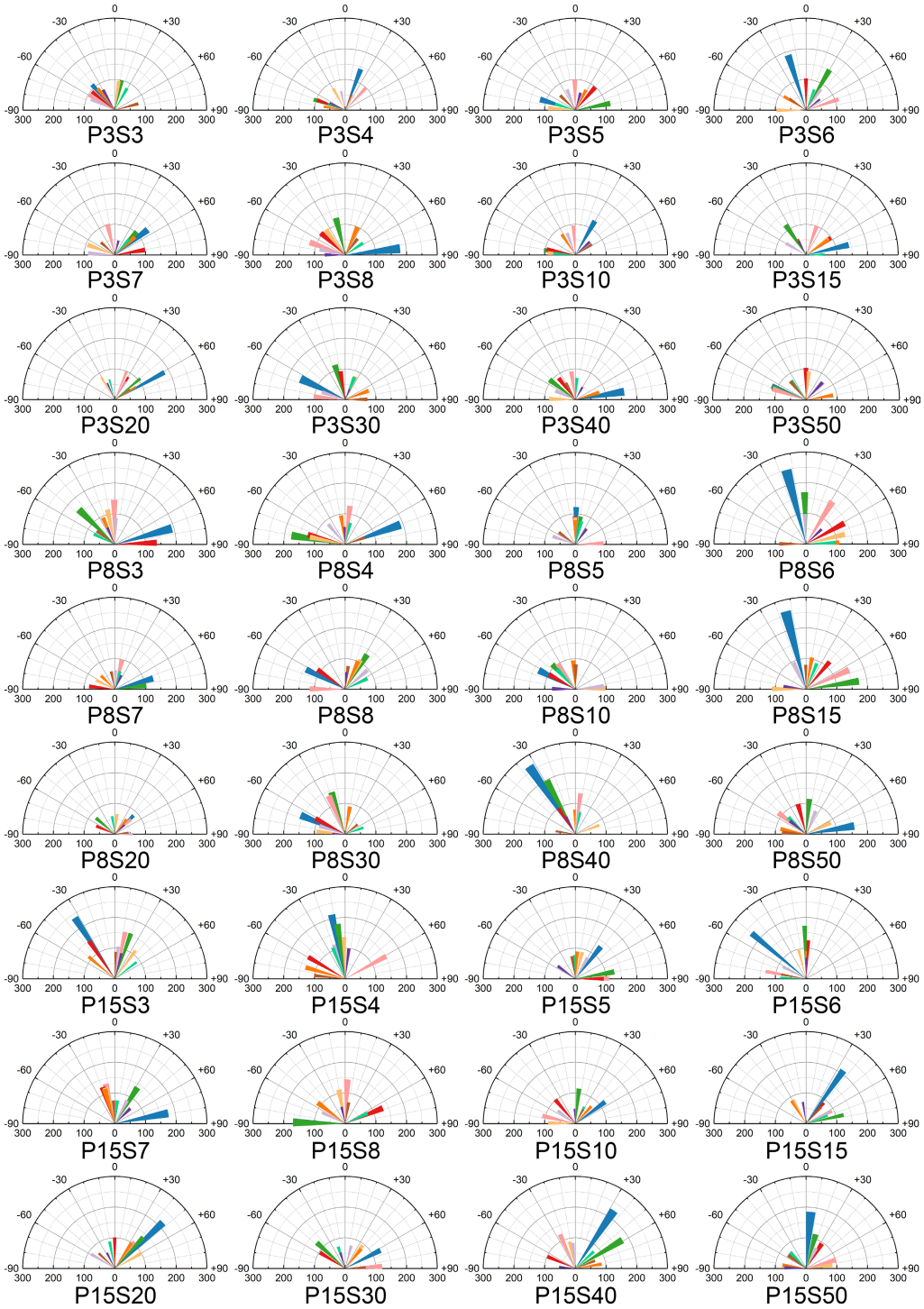

Fig. S16. Polar plots of the orientation angle with the cellular length (μm) of the cells on the micropillar patterns with a fixed pillar width of 3, 8, and 15 μm, i.e., P3, P8, and P15.

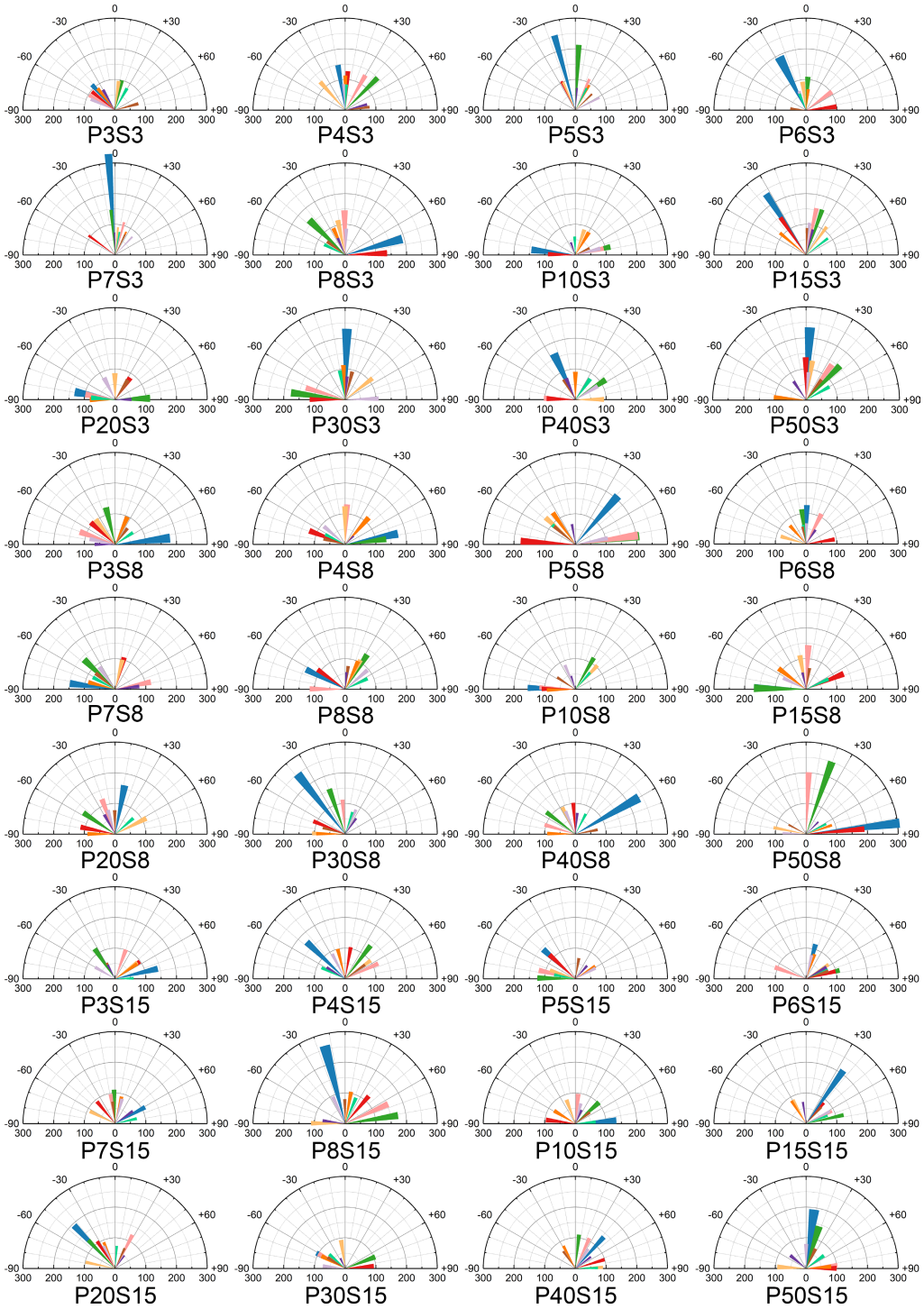

Fig. S17. Polar plots of the orientation angle with the cellular length (μm) of the cells on the micropillar patterns with a fixed space width of 3, 8, and 15 μm, i.e., S3, S8, and S15.

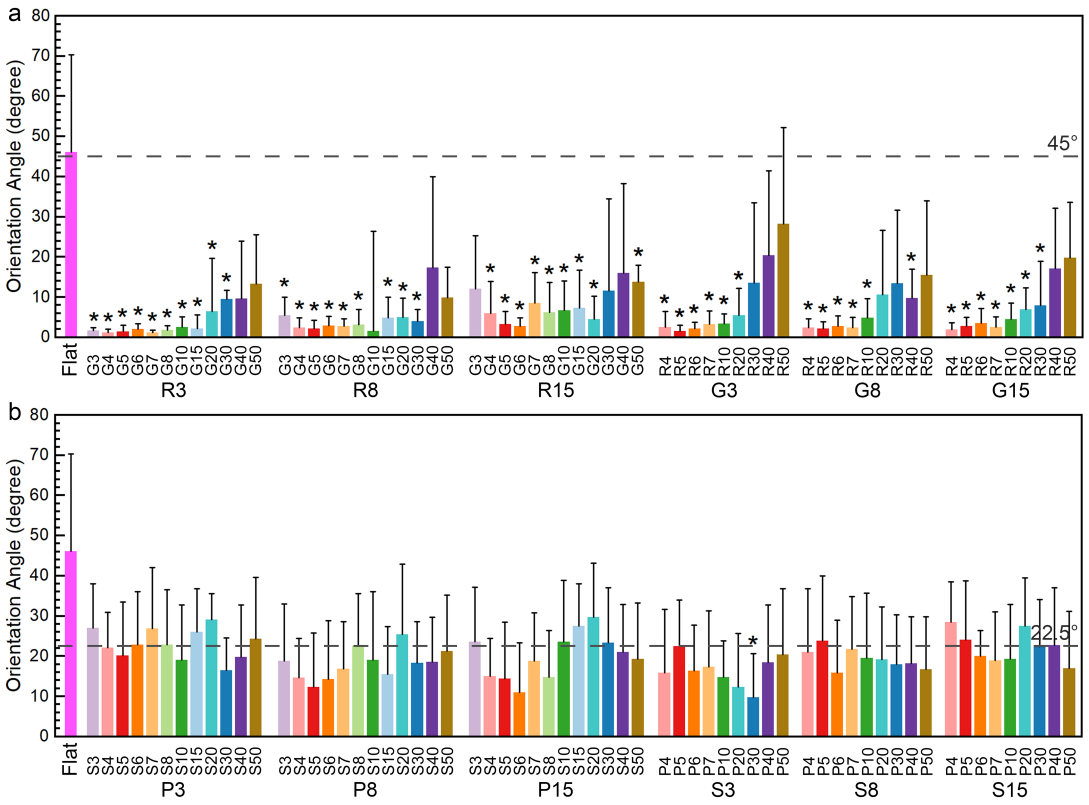

Fig. S18. Orientation angles of the cells on each pattern of the HA TopoChip: (a) microgrooves, (b) micropillars. $n = 10$, * $p < 0.05$.

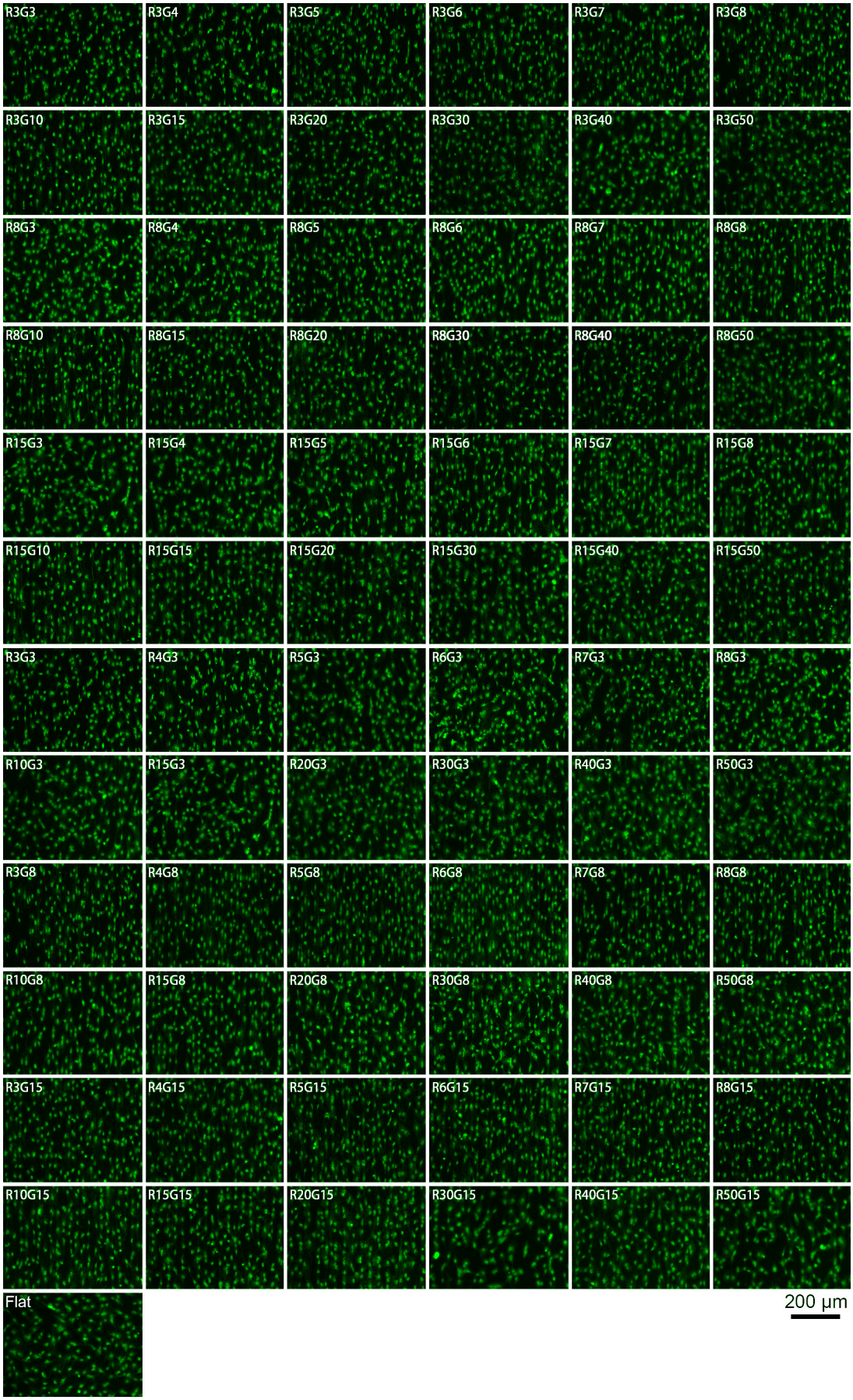

Fig. S19. IF images of ALP on the microgroove patterns and Flat.

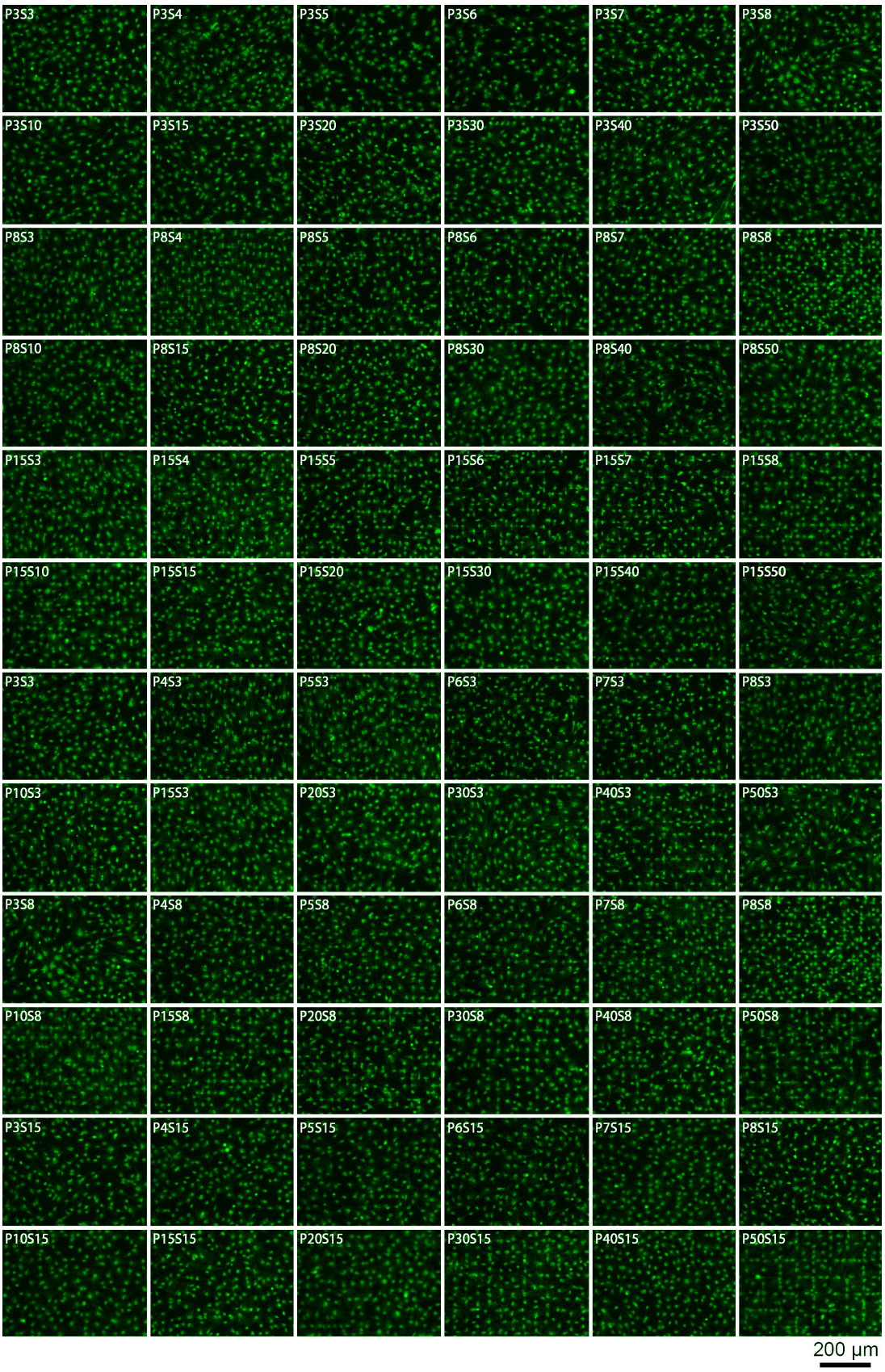

Fig. S20. IF images of ALP on the micropillar patterns.

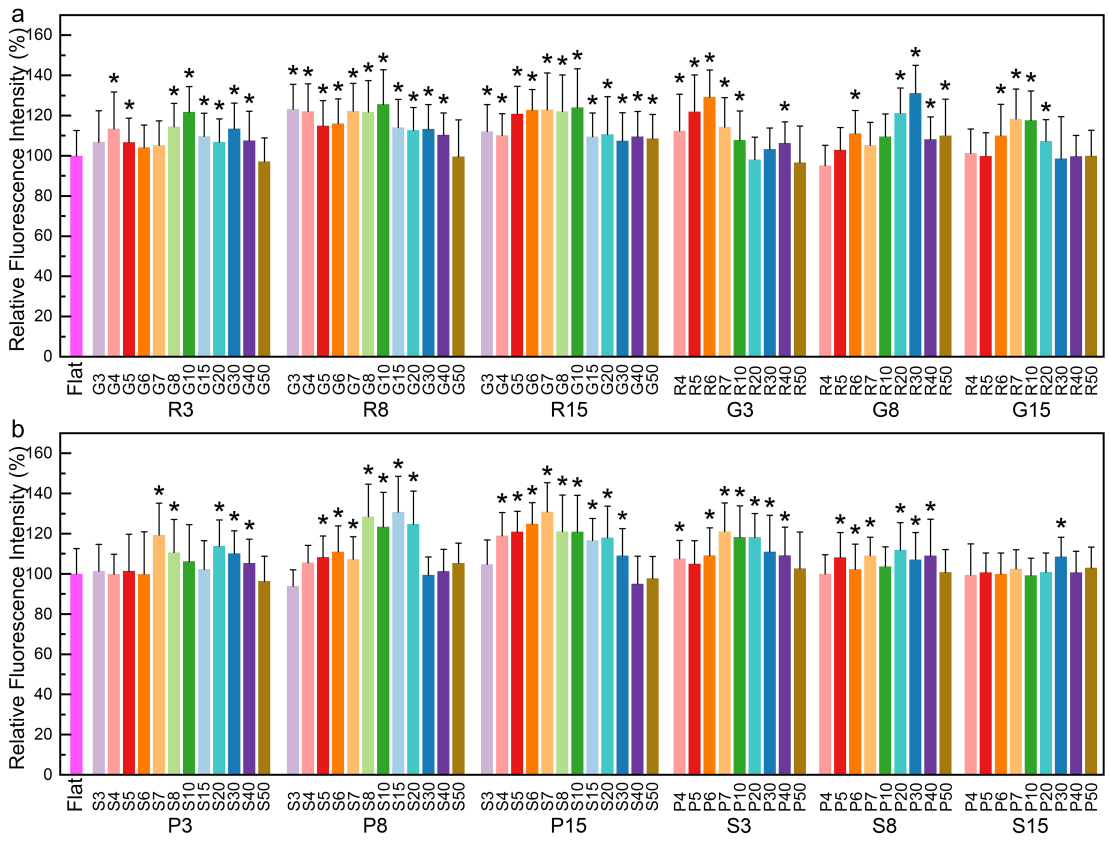

Fig. S21. Relative fluorescence intensity of ALP of rBMSCs osteogenically induced for 7 days on the groove (a) and pillar (b) patterns with the flat control.

Table S2. Patterns selected for in vitro and in vivo studies.

Pattern	Parameter	Application	Description
Groove	R6G3	Experimental	Highest ALP intensities in groove patterns
	R8G10	Experimental	
	R30G8	Experimental	
	R50G3	Low control	Lowest ALP intensity in groove patterns
Pillar	P8S8	Experimental	Highest ALP intensities in pillar patterns
	P8S15	Experimental	
	P15S7	Experimental	
	P15S40	Low control	Lowest ALP intensity in pillar patterns
Flat	—	Negative control	No pattern